Protein Science (2000), *9*:2477–2488. Cambridge University Press. Printed in the USA.

Enhancement by Mg^{2+} of domain specificity in Ca^{2+}-dependent interactions of calmodulin with target sequences

STEPHEN R. MARTIN, LAURA MASINO, AND PETER M. BAYLEY

Division of Physical Biochemistry, National Institute for Medical Research, The Ridgeway, Mill Hill, London NW7 1AA, United Kingdom

(RECEIVED June 13, 2000; FINAL REVISION September 15, 2000; ACCEPTED October 3, 2000)

Abstract

Mg^{2+} binds to calmodulin without inducing the changes in secondary structure that are characteristic of Ca^{2+} binding, or the exposure of hydrophobic surfaces that are involved in typical Ca^{2+}-dependent target interactions. The binding of Mg^{2+} does, however, produce significant spectroscopic changes in residues located in the Ca^{2+}-binding loops, and the Mg-calmodulin complex is significantly different from apo-calmodulin in loop conformation. Direct measurement of Mg^{2+} binding constants, and the effects of Mg^{2+} on Ca^{2+} binding to calmodulin, are consistent with specific binding of Mg^{2+}, in competition with Ca^{2+}. Mg^{2+} increases the thermodynamic stability of calmodulin, and we conclude that under resting, nonstimulated conditions, cellular Mg^{2+} has a direct role in conferring stability on both domains of apo-calmodulin. Apo-calmodulin binds typical target sequences from skeletal muscle myosin light chain kinase and neuromodulin with $K_d \sim 70$–90 nM (at low ionic strength). These affinities are virtually unchanged by 5 mM Mg^{2+}, in marked contrast to the strong enhancement of peptide affinity induced by Ca^{2+}. Under conditions of stimulation and increased $[Ca^{2+}]$, Mg^{2+} has a role in directing the mode of initial target binding preferentially to the C-domain of calmodulin, due to the opposite relative affinities for binding of Ca^{2+} and Mg^{2+} to the two domains. Mg^{2+} thus amplifies the intrinsic differences of the domains, in a target specific manner. It also contributes to setting the Ca^{2+} threshold for enzyme activation and increases the importance of a partially Ca^{2+}-saturated calmodulin–target complex that can act as a regulatory kinetic and equilibrium intermediate in Ca^{2+}-dependent target interactions.

Keywords: calcium binding; calmodulin; magnesium binding; optical spectroscopy; protein stability

The crucial molecular events in the translation of a Ca^{2+} signal into the activation of a cellular process are the binding of this ion by calmodulin (CaM), and the subsequent transition in CaM to a conformation that binds to and activates one or more of the family of Ca^{2+}–CaM-dependent enzymes (such as kinases) and channel proteins (Berridge et al., 1998). CaM shows great versatility in the range of targets with which it interacts in a Ca^{2+}-dependent manner, and the molecular basis of this versatility is evidently linked to the distinctive Ca^{2+}-binding properties of the two structural domains of CaM (see, e.g., Bayley et al., 1996; Peersen et al., 1997). The binding of Ca^{2+} to CaM has been studied extensively in vitro and comprises the binding of four Ca^{2+} ions, two to the C-terminal domain, with an average K_a of $\sim 6 \times 10^5$ M^{-1} and two to the N-terminal domain with average K_a of $\sim 6 \times 10^4$ M^{-1} at physiological ionic strength (Linse et al., 1991; Bayley et al., 1996). In vivo, this process occurs in response to the increase in resting $[Ca^{2+}]$ from <100 nM to >1 μM following cellular stimulation. It has long been recognized that cells contain relatively high levels of Mg^{2+} ($\sim$1–5 mM; Ebel & Gunther, 1980), and that the presence of this ion reduces the apparent affinity of both the CaM domains for Ca^{2+} (Haiech et al., 1981). There is considerable debate over the precise magnitude of the association constants of CaM for Mg^{2+} (generally reported to be in the range 10^2 to 10^4 M^{-1}; see Tsai et al. (1987) and references therein) and the relative specificity for the two domains. Controversy also remains over the relative affinity of individual sites and whether Mg^{2+} binds at additional (allosteric) sites distinct from the four Ca^{2+} binding sites (as inferred from binding studies; Milos et al., 1986; Gilli et al., 1998), or competes directly with Ca^{2+} for the binding sites in the EF-hand loops (as deduced from NMR studies; Seamon, 1980; Tsai et al., 1987; Ohki et al., 1997; Ouyang & Vogel, 1998). Finally, Mg^{2+} is known to be ineffective in replacing Ca^{2+} as the stimulus for Ca^{2+}-dependent enzyme activation, consistent with the inabil-

Reprint requests to: Peter M. Bayley, National Institute for Medical Research, Division of Physical Biochemistry, The Ridgeway, Mill Hill, London NW7 1AA, United Kingdom; e-mail: pbayley@nimr.mrc.ac.uk.

Abbreviations: CaM, *Drosophila melanogaster* calmodulin; sk-MLCK, skeletal myosin light chain kinase; 5,5′-Br_2BAPTA, 5,5′-dibromo-1,2-bis(2-aminophenoxy)ethane-*N,N,N′,N′*-tetraacetic acid.

ity of Mg^{2+} to cause hydrophobic exposure (Follenius & Gerard, 1984). This suggests that the two ions have important and specific effects on CaM conformation, which are translated into differences in the interaction with target sequences of susceptible enzymes. We therefore address the quantitative basis of how the presence of physiological [Mg^{2+}] affects and contributes to the domain specificity and versatility of Ca–CaM target interactions in the Ca^{2+}-dependent regulatory process of the eukaryotic cell.

In the present work, we extend previous applications to CaM of the methods of optical spectroscopy, absorption, near- and far-UV circular dichroism (CD) and fluorescence (Bayley et al., 1996) to study: (1) the effect of Mg^{2+} on the conformation of CaM, as judged by probes of secondary and tertiary structure; (2) the quantitation of Mg^{2+} binding to CaM by direct fluorometric titrations using WT CaM and a T26W mutant of syncam (Kilhoffer et al., 1992); (3) the effect of Mg^{2+} on the binding of Ca^{2+} to CaM using the 5,5′-Br_2BAPTA indicator method (Linse et al., 1991) and direct fluorometric titrations; and (4) the effect of Mg^{2+} on the interaction of CaM with target sequences from skeletal muscle myosin light chain kinase (sk-MLCK) and from neuromodulin, in the presence and absence of Ca^{2+}.

We find that the effect of Mg^{2+} depends on the Ca^{2+} sensitivity of the CaM–target interaction. The higher affinity of Mg^{2+} for N-domain compared with C-domain increases the apparent relative weakness in the Ca^{2+}-dependent target affinity of the N-domain, under conditions of cellular stimulation and [Ca^{2+}] increase. Numerical simulations show that this factor significantly enhances the specificity of the Ca^{2+}-dependent target affinity for the C-domain of CaM in a partially Ca^{2+}-saturated intermediate, as previously postulated (Bayley et al., 1996). We conclude that intracellular Mg^{2+} has an effective role in modulating the relative affinities of Ca^{2+}-dependent target interactions. Numerical simulations of the competitive binding of Mg^{2+} and Ca^{2+} to CaM in the presence of target sequences illustrate how Mg^{2+} contributes significantly to the unique versatility of the regulatory Ca^{2+}-dependent interactions of CaM.

Results and discussion

Conformational effects of Mg^{2+}

Interpreting changes in the optical properties of apo-CaM induced by adding metal ions (or, indeed, by changing solution conditions such as pH, ionic strength, or temperature) is complicated by the fact that the C-domain of apo-CaM is intrinsically unstable, particularly at low ionic strengths. The free energies for unfolding of the C-domain (ΔG°_{20}) are ~0.5 kcal/mol (no KCl) and ~1.5 kcal/mol (100 mM KCl); the N-domain is significantly more stable (ΔG°_{20} ~3.55 kcal/mol in 100 mM KCl) (Masino et al., 2000). Thus, the far-UV CD spectrum of apo-CaM recorded in 25 mM Tris at 20 °C (Fig. 1A, curve B) is significantly less intense than those recorded in 25 mM Tris at 2 °C (curve B*) or in 25 mM Tris containing 200 mM KCl at 20 °C (curve K). These differences are consistent with the C-domain (~30% unfolded in 25 mM Tris at 20 °C) being stabilized by decreasing the temperature or by increasing the ionic strength. (Note: the N-domain of apo-CaM, which accounts for ~55% of the total CD signal (Martin & Bayley, 1986), is not significantly unfolded in the absence of KCl at 20 °C.) Addition of Mg^{2+} to apo-CaM in 200 mM KCl has no effect on the far-UV CD spectrum. Adding Mg^{2+} to apo-CaM in 25 mM Tris increases the intensity (curve Mg) but only to that obtained by increasing [KCl] or by lowering the temperature. We conclude, therefore, that the secondary structure of Mg-CaM is closely similar to that of apo-CaM at physiological ionic strengths, and that the effect of Mg^{2+} in low ionic strength buffers may be attributed to Mg^{2+} stabilizing the C-domain of CaM through preferential binding to the native folded state. The well-known effect of Ca^{2+} (curve Ca) on the far-UV CD intensity is much larger (Martin & Bayley, 1986).

The absorption, near-UV-CD, and Tyr138 fluorescence spectra of apo-CaM recorded in 25 mM Tris (Fig. 1B–D) show intensities that are intermediate between those recorded in 200 mM KCl and those recorded under denaturing conditions (typically 6 M GuHCl). In each case the intensity measured in 25 mM Tris is consistent with the C-domain of apo-CaM (containing Tyr138, the major contributor to these spectra) being ~30% unfolded under these conditions. The absorption (Fig. 1C) and near-UV CD (Fig. 1B) spectra of CaM in the presence of 10 or 20 mM $MgCl_2$ are closely similar to those of apo-CaM recorded in 200 mM KCl. In neither case is the characteristic Ca^{2+}-induced change observed; suggesting that Mg^{2+} binding has significantly less effect on the tertiary structure of CaM. In the case of Tyr138 fluorescence (Fig. 1D), the addition of Mg^{2+} produces an increase in fluorescence similar to, but smaller than that produced by Ca^{2+} (cf. Kilhoffer et al., 1981). Because the CD results show that Mg^{2+} binding does not change the secondary or tertiary structure of CaM, this must mean that the signal from Tyr138 derives from occupancy of site IV by Mg^{2+} and is not a conformational effect (cf. Seamon, 1980).

The results reported here are consistent with NMR studies in which it was concluded that the effects of Mg^{2+} on CaM are limited to the immediate vicinity of the metal–ion-binding site (Seamon, 1980; Tsai et al., 1987; Ohki et al., 1997; Ouyang & Vogel, 1998). Magnesium therefore should not cause the hydrophobic surface exposure characteristic of Ca^{2+} binding. We have compared hydrophobic exposure in Ca-CaM with that in Mg-CaM in two ways. The hydrophobic probe TNS binds to Ca-CaM (but not to apo-CaM) and generates intense fluorescence; we could not observe this TNS binding in the presence of 10 mM $MgCl_2$ (cf. Follenius & Gerard, 1984). Similarly, we have employed two cysteine mutants of CaM (S38C and N111C) labeled with the fluorescent probe dansyl maleimide. In both cases the addition of Ca^{2+} to the labeled apo-CaM mutant causes a large blue shift in the fluorescence, consistent with the probe interacting with exposed hydrophobic surfaces on the protein. This effect is not observed upon the addition of 10 mM $MgCl_2$ to either of the mutant proteins in the apo state.

Direct measurement of Mg^{2+} binding to the C- and N-terminal domains of calmodulin

Binding of Mg^{2+} to the C-terminal domain of CaM has been monitored using the changes in Tyr138 fluorescence described in Figure 1D. Figure 2A shows Mg^{2+} titrations of apo-CaM performed in the presence of 0, 25, and 100 mM KCl. The final intensity at saturating [Mg^{2+}] is the same at all [KCl], confirming that there is no direct effect of KCl on the Tyr138 fluorescence of Mg-CaM. The signal at the starting point is higher in the absence of KCl because the C-domain of CaM is partly unfolded under these conditions and unfolding leads to an increase in the fluorescence (see Fig. 1D). The free [Mg^{2+}] at the midpoints of the fluorescence changes correspond to $K^{C}_{av(Mg)}$ values of 580, 330, and

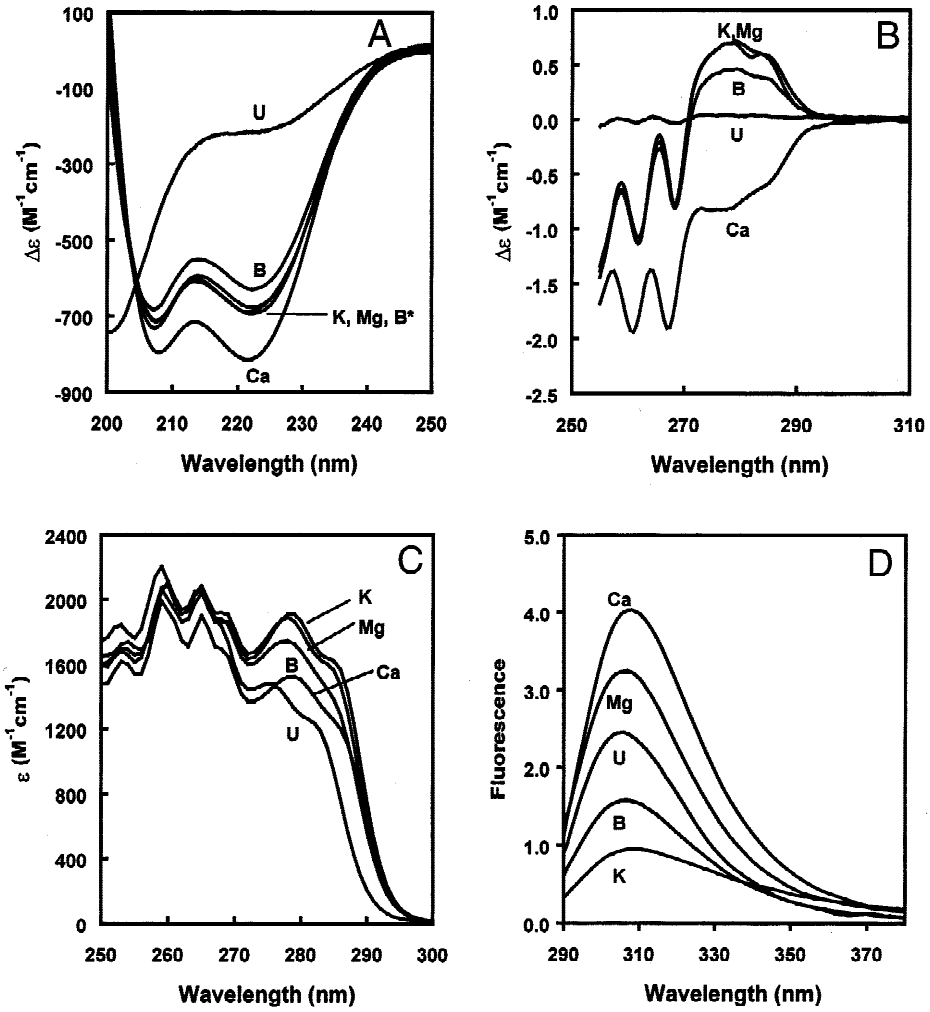

Fig. 1. Optical spectra of CaM. (**A**) Far-UV CD, (**B**) near-UV CD, (**C**) absorption, and (**D**) fluorescence (280 nm excitation) spectra. All measurements were made at 20 °C in 25 mM Tris, pH 8.0 (unless otherwise noted). The symbols denote spectra recorded in buffer alone (B), in buffer alone at 2 °C (B*), in buffer plus 200 mM KCl (K), in buffer plus 1 mM $CaCl_2$ (Ca), and in buffer plus 20 mM $MgCl_2$ (Mg). Spectra for the unfolded form (U) were obtained in 10 mM Hepes (pH 7.5) at 75 °C for far-UV CD and in buffer containing 6M GuHCl in all other cases.

175 M^{-1}, respectively (cf. Drabikowski et al., 1982). The corresponding values for calcium (i.e., $K^{C}_{av(Ca)}$) are given in Table 1.

Binding of Mg^{2+} to the N-terminal domain of CaM has been monitored using Mg^{2+}-induced changes in the tryptophan fluorescence of the T26W syncam mutant (Kilhoffer et al., 1992). To confirm that the changes in Trp26 fluorescence monitor the binding of the metal ion to the N-domain of CaM, we performed a control titration of apo-T26W-syncam with Ca^{2+} in the presence of 100 mM KCl (Fig. 2B). This gave a direct estimate of $K^{N}_{av(Ca)}$ as $\sim 4.7 \times 10^4$ M^{-1}; in reasonable agreement with a value of $\sim 6 \times 10^4$ M^{-1} deduced for WT CaM (Linse et al., 1991; Bayley et al., 1996).

Figure 2C shows Mg^{2+} titrations of apo-T26W-syncam performed in the presence of 0, 25, and 100 mM KCl. The free $[Mg^{2+}]$ at the midpoints of the fluorescence changes correspond to $K^{N}_{av(Mg)}$ values of 2,700, 1,250, and 570 M^{-1}, respectively. The corresponding values for Ca^{2+} binding to WT-CaM (i.e., $K^{N}_{av(Ca)}$) are given in Table 1. The effect of ionic strength on the metal ion affinity appears to be significantly smaller for Mg^{2+} than for Ca^{2+}. This is, however, difficult to quantify because of the ionic strength contribution from Mg^{2+} itself.

Magnesium/calcium competition

The effects of Mg^{2+} on Ca^{2+} binding have been assessed by the indicator method using Ca^{2+} titrations of CaM in the presence of the chelator 5,5′-Br_2BAPTA and by direct fluorescence titrations using Tyr138 (WT-CaM) or Trp26 (T26W-syncam).

Calcium titrations of apo-CaM using the chromophoric chelator 5,5′-Br_2BAPTA were performed in the presence of 0, 1, 2, 5, and 10 mM $MgCl_2$, with the ionic strength maintained at a constant value (0.1 M) by appropriate variation in the total KCl concentration. The titrations are shown in Figure 3A, and the results of the analyses are presented in Table 2. The products K_1K_2 and K_3K_4 (which reflect binding to the C- and N-terminal domains of CaM, respectively—see Materials and methods) are both reduced as $[Mg^{2+}]$ is increased. The effect of Mg^{2+} is clearly greatest in the case of K_3K_4, which falls below the detection limit of this chelator

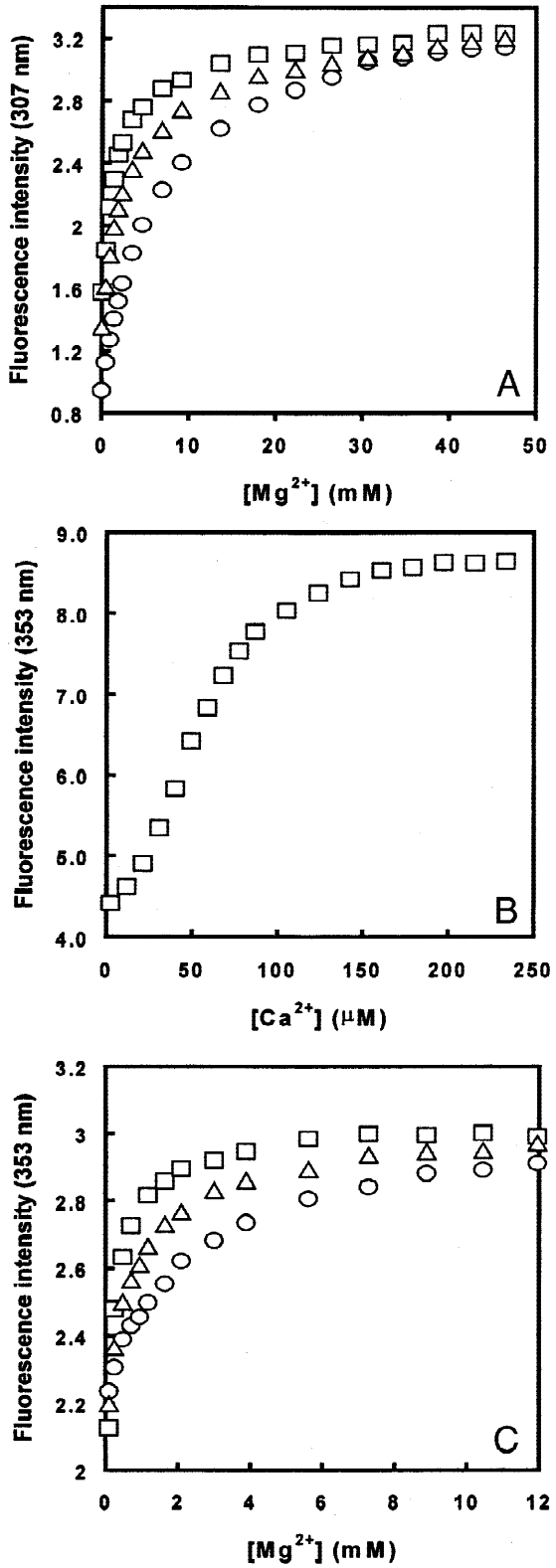

Fig. 2. Interaction of Mg^{2+} and Ca^{2+} with CaM and T26W-syncam. **A:** Magnesium titrations of apo-CaM (7.0 μM) in the presence of 0 (□), 25 (△), and 100 (○) mM KCl. The measurements were made at 20 °C in 25 mM Tris (pH 8.0). Excitation was at 280 nm. **B:** Calcium titration of apo-T26W-syncam (10.7 μM). **C:** Magnesium titrations of apo-T26W-syncam (5.35 μM) in the presence of 0 (□), 25 (△), and 100 (○) mM KCl. Excitation was at 290 nm. All measurements were made at 20 °C in 25 mM Tris (pH 8.0).

Table 1. *Average Mg^{2+} and Ca^{2+} affinities of the N- and C-terminal domains of CaM*

[KCl] (mM)	$K^{C}_{av(Mg)}$ [a] (M^{-1})	$K^{C}_{av(Ca)}$ [b] (M^{-1})	$K^{N}_{av(Mg)}$ [c] (M^{-1})	$K^{N}_{av(Ca)}$ [b] (M^{-1})
0	580	2.0×10^7	2,700	3.5×10^6
25	330	2.5×10^6	1,250	3.5×10^5
100	175	5.0×10^5	570	6.0×10^4

[a] Measured using Tyr138 fluorescence (WT CaM).
[b] $K^{C}_{av(Ca)}$ and $K^{N}_{av(Ca)}$ were calculated from data in Linse et al. (1991) as described in Materials and methods.
[c] Measured using Trp26 fluorescence (T26W syncam).

at $[Mg^{2+}] = 10$ mM. The calculated $K_{av(Mg)}$ values are clearly rather sensitive to errors in the product of the stoichiometric association constants (typically 0.15 log units). Nevertheless, the calculated values are closely similar to the average values measured using direct fluorescence titrations of Tyr138 (C-domain, WT-CaM) and Trp26 (N-domain, T26W-syncam).

Because the responses of Tyr138 fluorescence (WT-CaM) and Trp26 fluorescence (T26W-syncam) are substantially greater for Ca^{2+} binding (see Figs. 1D, 2B,C) it is possible to use these signals to measure apparent Ca^{2+} affinities in the presence of Mg^{2+}. Ca^{2+} titrations in the presence of 0, 5, and 10 mM Mg^{2+} are shown in Fig. 3B (Tyr138) and 3C (Trp26). The analysis of these experiments is presented in Table 3. Given the necessary approximations involved in these calculations, the estimated $K_{av(Mg)}$ values are in good agreement with those derived from Mg^{2+} effects on the stoichiometric association constants (Table 2).

Effect of magnesium on interaction of CaM with target sequences

To assess the effects of Mg^{2+} on the interaction of CaM with typical target sequences, we have used two Trp-containing peptides, WFF_p (18 residues) and NM2 (19 residues). WFF_p corresponds to the major part of the CaM-binding domain of sk-MLCK, and is bound to Ca-CaM with very high affinity at physiological ionic strengths ($K_d \sim 2$ pM; Martin et al., 1999). NM2 corresponds to part of the CaM-binding domain of neuromodulin (with an I4W substitution) and is bound to Ca-CaM with significantly lower affinity ($K_d \sim 30$ nM). Stoichiometric Ca^{2+} association constants measured in the presence of WFF_p (or NM2) are $\log K_1 = 6.86$ (6.45), $\log K_2 = 8.01$ (7.19), $\log K_3 = 6.97$ (5.17), and $\log K_4 = 6.93$ (5.43).

The analyses presented here are based on the fact that the Trp fluorescence spectrum of the peptide depends on the nature of the CaM species with which it interacts. This is illustrated in Figure 4A, which shows the spectra of WFF_p in the absence of CaM ($\lambda_{em} \sim 356$ nm), in the presence of apo-CaM ($\lambda_{em} \sim 344$ nm), in the presence of CaM plus 10 mM Mg^{2+} ($\lambda_{em} \sim 336$ nm), and in the presence of CaM plus 1 mM Ca^{2+} ($\lambda_{em} \sim 332$ nm). These different signals allow the determination of K_ds for the interaction of the peptide with CaM in the presence and absence of Mg^{2+} or Ca^{2+}. Typical titrations of 2.25 μM WFF_p with CaM are shown in Figure 4B. The K_ds for the interaction with CaM in the absence of calcium are ~88 nM (at [KCl] = 0), ~720 nM (at [KCl] = 30 mM), and ~1.4 μM (at $[Mg^{2+}] = 10$ mM, [KCl] = 0). In the presence

of Ca^{2+} (25 μM), the K_d for this peptide is much too low to be measured by direct fluorometric titration at the concentrations used here. Interestingly, however, the same curve is obtained when this titration is repeated in the presence of 10 mM Mg^{2+}. Calculation shows that any effect of Mg^{2+} in reducing the K_d must be less than 100-fold. Because of the very low K_d, it is not possible to quantify the effect of Mg^{2+} in this assay. We have therefore performed similar studies with the peptide NM2, which binds to Ca-CaM with much lower affinity, and any effects of Mg^{2+} should be more readily observable. The results of these experiments are summarized in Table 4. Several features may be noted.

1. The interaction of both peptides with apo-CaM is strongly ionic strength dependent; thus, the K_d in 30 mM KCl is approximately one order of magnitude greater than that in the absence of KCl (cf. Tsvetkov et al., 1999).

2. Mg-CaM binds either of the peptides more weakly than does apo-CaM. At the two ionic strengths examined, the K_d for the peptide measured for Mg-CaM is between two- and fivefold higher than that of apo-CaM. The effect appears to be somewhat greater for NM2 than for WFF_p. Although the effect is small, it would serve to minimize any CaM–target interactions occurring at resting calcium concentrations. Because the structures of the complexes formed with apo-CaM are not known the origin of the effect is unclear. However, as such interactions appear to be primarily electrostatic in nature (Tsvetkov et al., 1999), it may be that the binding of Mg^{2+} (partially) screens some important negative charges on CaM.

3. The effect of 5 mM Mg^{2+} on the apparent affinity of Ca-CaM for NM2 is small, even at the lowest $[Ca^{2+}]$ employed (10 μM). At this $[Ca^{2+}]$ the K_d for Ca-CaM in the absence of Mg^{2+} is also slightly increased compared with values measured at higher $[Ca^{2+}]$. Part of the effect of Mg^{2+} may be attributable to the small ionic strength difference in these experiments.

Two testable predictions emerge from these results.

1. Because the affinity of the peptides for CaM is not increased in the presence of Mg^{2+} (in fact, it is slightly decreased) then it should also be true that the affinity of an apo-CaM-peptide complex for Mg^{2+} is similar to that of apo-CaM. This was confirmed using a fluorescence titration of the apo-CaM-WFF_p complex with Mg^{2+} in the absence of KCl (Fig. 4C). The midpoint of the titration is ~0.4 mM, corresponding to an apparent binding constant for Mg^{2+} to the complex of the order of 2,500 M^{-1} (cf. values for apo-CaM itself, $K^N_{av(Mg)}$ = 2,700 M^{-1} and $K^C_{av(Mg)}$ = 580 M^{-1}).

2. Because the Ca^{2+} affinity of CaM is greatly increased in the presence of target sequences, only low concentrations of Ca^{2+}

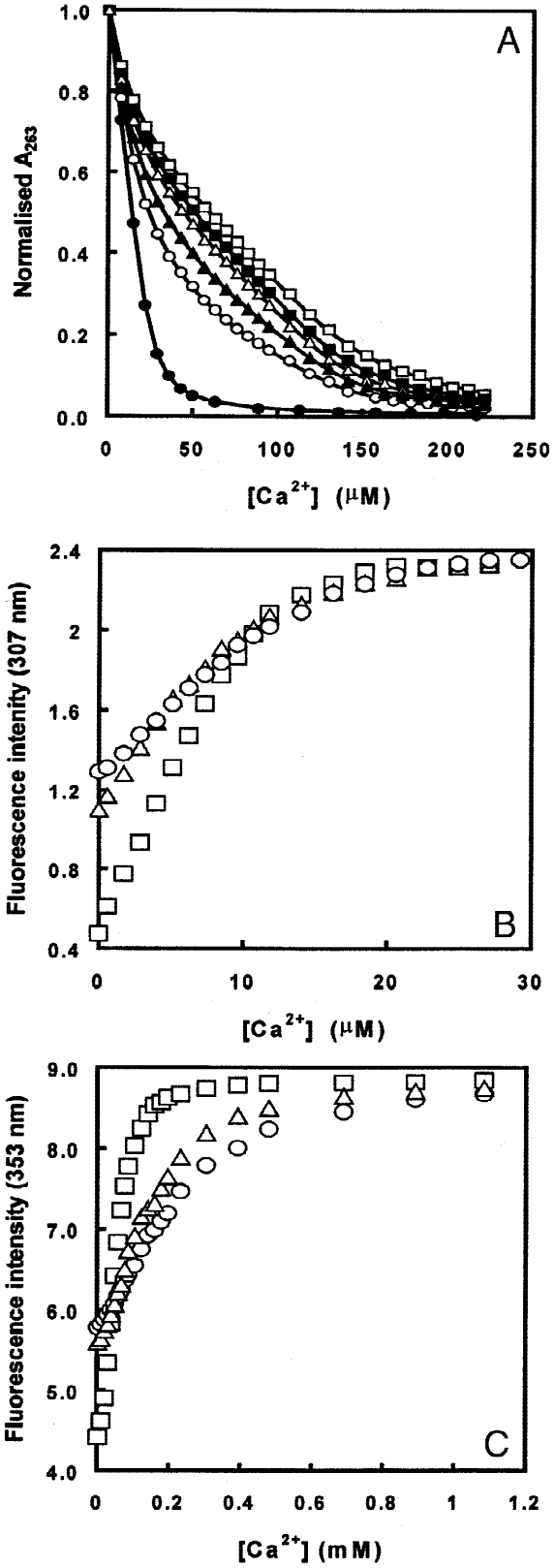

Fig. 3. Magnesium/calcium competition. **A:** Ca^{2+} titrations of 26.0 μM 5,5′-Br_2BAPTA plus 48 μM apo-CaM in the presence of 0 (□), 1 (■), 2(△), 5 (▲), and 10 (○) mM $MgCl_2$. A control titration with no CaM (●) is shown for comparison. The measurements were made at 20 °C in 10 mM Tris, 100 mM KCl (pH 8.0). The total absorbance change has been normalized to facilitate comparison of the curves. **B:** Ca^{2+} titrations of apo-CaM (3.5 μM) in the presence of 0 (□), 5 (△), and 10 (○) mM $MgCl_2$ monitored using Tyr138 fluorescence. Excitation was at 280 nm. Measurements were made at 20 °C in 25 mM Tris, 100 mM KCl (pH 8.0). **C:** Ca^{2+} titrations of apo-T26W-syncam (10.7 μM) in the presence of 0 (□), 5 (△), and 10 (○) mM $MgCl_2$ monitored using Trp26 fluorescence. Excitation was at 290 nm. Measurements were made at 20 °C in 25 mM Tris, 100 mM KCl (pH 8.0).

Table 2. *Ca^{2+} titrations of apo-CaM in the presence of 5,5′-Br_2BAPTA at different [Mg^{2+}]*

[Mg^{2+}] (mM)	Measured $\log(K_1K_2)$	Measured $K^C_{av(Ca)}$ (M^{-1})[a]	Calculated $K^C_{av(Mg)}$ (M^{-1})[b]	Measured $\log(K_3K_4)$	Measured $K^N_{av(Ca)}$ (M^{-1})[c]	Calculated $K^N_{av(Mg)}$ (M^{-1})[b]
0	11.55	5.95×10^5	—	9.61	6.38×10^4	—
1	11.44	5.25×10^5	135	9.36	4.78×10^4	333
2	11.28	4.37×10^5	182	8.89	2.78×10^4	649
5	10.82	2.57×10^5	264	8.66	2.14×10^4	397
10	10.71	2.26×10^5	163	—	—	—

[a]Calculated as $(K_1K_2)^{0.5}$.
[b]Calculated as described in Materials and methods.
[c]Calculated as $(K_3K_4)^{0.5}$.

should be required to displace Mg^{2+} from the Mg-CaM-peptide complex. This was confirmed by the observation (data not shown) that only low calcium concentrations (<12 μM) were required to convert the Mg-CaM-WFF_p spectrum to the Ca-CaM-WFF_p spectrum in the presence of 10 mM Mg^{2+}.

Analysis of Mg^{2+} effects on Ca^{2+}-dependent CaM–target interactions

The effect of Mg^{2+}on Ca^{2+}-dependent interaction of CaM with typical target sequences has been assessed by measuring affinities under specified Ca^{2+}, Mg^{2+} concentration conditions. Stoichiometric association constants for Ca^{2+} binding in the presence of WFF_p and NM2 have also been measured. In the absence of target, the products K_1K_2 and K_3K_4 reflect binding to the C- and N-terminal domains of CaM, respectively (Linse et al., 1991). In the presence of WFF_p, both these products are increased, showing that both domains undergo a Ca^{2+}-dependent interaction with different parts of the target. The affinities for Ca^{2+} in the presence of NM2 show that the product K_1K_2 is increased significantly more than K_3K_4, indicating that it is the C-domain that is mainly involved in the Ca^{2+}-dependent interaction. Calcium titrations of apo-CaM plus WFF (Martin et al., 1996) and NM2 (not shown) show that the near-UV CD signals associated with the peptide Trp and Tyr138 are >75% complete upon the addition of two Ca^{2+} ions. This shows that the first two Ca^{2+} bind principally to the C-terminal domain of CaM (as with CaM in the absence of target), which interacts with the N-terminal portion of the WFF_p (or NM2) sequences to form the Ca_2-CaM-WFF_p and Ca_2-CaM-NM2 complexes. We conclude that the products K_1K_2 and K_3K_4 also reflect C- and N-domain binding in the presence of these target sequences.

Table 3. *Fluorescence titrations in the presence of different [Mg^{2+}]*

[Mg^{2+}] (mM)	Measured $K^C_{av(Ca)}$ [a]	Calculated $K^C_{av(Mg)}$ [b]	Measured $K^N_{av(Ca)}$ [c]	Calculated $K^N_{av(Mg)}$ [b]
0	5.55×10^5	—	4.67×10^4	—
5	3.12×10^5	167	9.90×10^3	745
10	2.22×10^5	150	5.52×10^3	748

[a]Measured using Tyr138 fluorescence (WT CaM). The $[Ca]_{0.5}$ values used in the calculation of $K^C_{av(Ca)}$ were corrected for minor N-domain occupancy, which was estimated to be ~3% at the midpoint [Ca^{2+}] observed in the experiment with no Mg^{2+}.
[b]Calculated as described in Materials and methods.
[c]Measured using Trp26 fluorescence (T26W syncam). The $[Ca]_{0.5}$ values used in calculation of $K^N_{av(Ca)}$ were corrected by assuming that the C-domain was at least 97% occupied at the midpoint [Ca^{2+}] observed in the experiment with no Mg^{2+}.

We model the behavior of this system of CaM, Ca^{2+}, Mg^{2+}, and peptide by calculating the concentrations of appropriate species as a function of [Ca^{2+}]. The interrelationships of the main species are shown in Scheme 1. We adopt a simple model in which K_1 and K_2 for the interaction of Ca^{2+} with a CaM–peptide species are reduced by $1/(1 + K^C_{av(Mg)}[Mg^{2+}])$, while the corresponding K_3 and K_4 are reduced by $1/(1 + K^N_{av(Mg)}[Mg^{2+}])$. We have confirmed the validity of this assumption by measuring stoichiometric Ca^{2+} association constants for CaM in the presence of NM2 in a buffer containing 5 mM $MgCl_2$. The values ($\log K_1 = 5.93$, $\log K_2 = 7.05$, $\log K_3 = 4.55$, and $\log K_4 = 4.66$) correspond to reductions by factors of 3.3 (K_1), 1.4 (K_2), 4.2 (K_3), and 5.9 (K_4), which agree moderately well with predicted values (see above) of ~1.9 (K_1 and K_2) and ~3.85 (K_3 and K_4). Nevertheless, this is a minimal illustrative model since the effects of Mg^{2+} are attributed solely to competition with Ca^{2+}. Thus, any Mg^{2+}-induced changes in target affinity are ignored; i.e., it is implicitly assumed that Mg_x-CaM and apo-CaM have the same affinity for the target, and the same relationship holds for Mg_xCa_y-CaM and Ca_y-CaM. If Mg_x-CaM actually binds the target more strongly than does apo-CaM, then the enhancement of target affinity by Ca^{2+} binding could be attenuated even further than indicated. These calculations allow an illustration of the principles by which Mg^{2+} can exert a significant influence on target interactions, despite the limited ability of Mg^{2+} to produce conformational changes in CaM.

For simplicity, we show only the concentrations of species with 0, 2, and 4 bound Ca^{2+} ions. Figures 5A and 5B shows that the saturation curve for the appearance of Ca_4-CaM is shifted from pCa 4.8 to pCa 4.2 in the presence of 5 mM Mg^{2+}. At the same time, the behavior of the intermediate species Ca_2-CaM changes significantly, being maximally 72% of total CaM at pCa 5.3 (Fig. 5A) and 82% at pCa 4.9 (Fig. 5B). Thus, an increased amount of CaM is present at this intermediate, and this exists at a higher [Ca^{2+}]. In the presence of peptide WFF_p, all four stoichiometric association constants are significantly increased. Hence, the saturation curve is displaced from pCa 4.8 (Fig. 5A) to pCa 6.3 (Fig. 5C) by the peptide, and in the presence of Mg^{2+}, from pCa 4.2 (Fig. 5B)

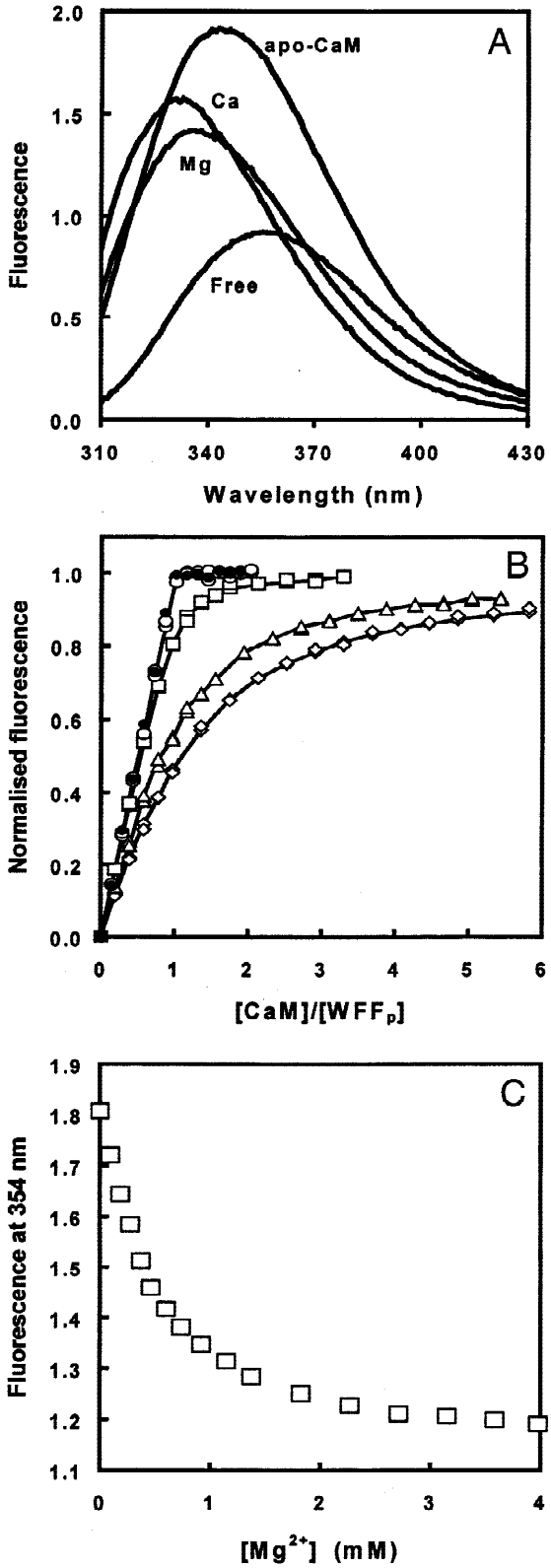

Fig. 4. Effect of Mg^{2+} on the interaction of CaM with a target peptide. **A:** Fluorescence spectra of WFF_p (6.7 μM) and its complexes with apo-CaM, Ca-CaM, and Mg-CaM. **B:** Titrations of WFF_p (2.3 μM) with CaM in buffer alone (□), 250 μM $CaCl_2$ (●), 100 μM $CaCl_2$ + 10 mM $MgCl_2$ (○), 30 mM KCl (△), and 10 mM $MgCl_2$ (◇). **C:** Titration of apo-CaM-WFF_p complex (6.7 μM) with $MgCl_2$. All measurements were made at 20 °C in 25 mM Tris (pH 8.0). Excitation was at 290 nm.

Table 4. *Peptide affinities in the presence of different concentrations of Ca^{2+}, Mg^{2+}, and KCl*

$[Ca^{2+}]$ (μM)	$[Mg^{2+}]$ (mM)	[KCl] (mM)	K_d (WFF_p) (nM)	K_d (NM2) (nM)
0	0	0	88 (12)	70 (12)
0	5	0	720 (80)	780 (120)
0	10	0	1,400 (150)	2,500 (400)
0	0	15	420 (70)	260 (45)
0	0	30	750 (120)	490 (120)
0	0	100	35,000 (5,000)	39,000 (8,000)
10	0	100	nd[a]	71 (7)
26	0	100	nd	31 (9)
100	0	100	nd	34 (6)
1,000	0	100	0.002[b]	31 (6)
10	5	100	nd	158 (18)
26	5	100	nd	75 (12)
100	5	100	nd	72 (14)

[a]nd, not determined.
[b]From Martin et al. (1999).

to pCa 5.8 (Fig. 5D). Again, the maximal proportion of the intermediate species (Ca_2-CaM-WFF_p) increases, from 42% at pCa 6.6 (Fig. 5C) to 61% at pCa 6.2 (Fig. 5D). The intermediate species is present in a significantly greater proportion of the total CaM, and this is achieved optimally at the expense of an increase in the $[Ca^{2+}]$ of approximately threefold (from pCa ~6.3 to ~5.8); i.e., at a level (~1 μM) only slightly above resting $[Ca^{2+}]$. Thus, the effect of Mg^{2+} is to moderate the effect of peptide in enhancing the apparent affinity of CaM for Ca^{2+} and setting the range over which formation of the Ca_4-CaM-target complex is formed and, hence, by analogy over which enzyme activation by Ca^{2+} is generally expected to occur.

An interesting contrast is presented by the peptide NM2, based on the target sequence of neuromodulin, which shows Ca^{2+}-independent interaction with CaM. The main category of such targets includes proteins with the IQ motif, IQxxxRGxxxR, as reviewed by Houdusse et al. (1996). These include the (generally) multiple IQ sequences of unconventional myosins, and the single IQ motifs of the neuronal proteins, neuromodulin (GAP43), neurogranin (RC3), and Pep19. Neuromodulin itself binds CaM somewhat more strongly in the absence of Ca^{2+}; we report the affinity for a modified version of the target sequence with the I4W substitution (NM2) in the presence and absence of Ca^{2+}: the affinity for CaM is seen to be ionic strength dependent in the absence of Ca^{2+} (Table 4). The affinity for the target sequence is enhanced only 1,000-fold in the presence of Ca^{2+}, in marked contrast to the case of sk-MLCK. The species plots show that the affinity of NM2 is such that in the absence of Mg^{2+} (Fig. 5E), the intermediate species Ca_2-CaM-NM2 is formed to ~75% at pCa = 6.1: the effect of 5mM Mg^{2+} (Fig. 5F) is to increase the maximum amount of Ca_2-CaM-NM2 to ~83% at pCa = 5.6, with a significant broadening of the $[Ca^{2+}]$ range over which this species is significantly populated. At the same time, the midpoint for full saturation increases from pCa ~ 5.1 to pCa ~ 4.5, representing the increased $[Ca^{2+}]$ required to effect full formation of Ca_4-CaM-NM2. It may be noted that the saturation curve is also a function of the absolute concentration of CaM, for a given [NM2]/[CaM] ratio, and, at higher values, the saturation curve in the presence of NM2 be-

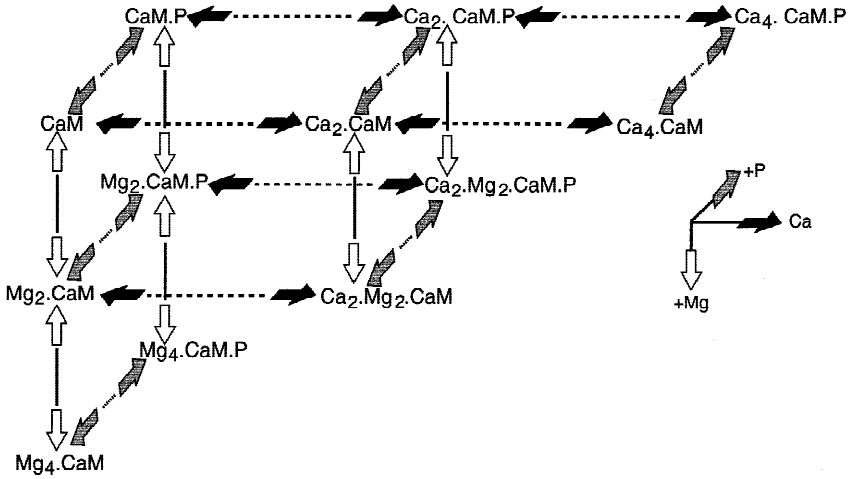

Scheme 1. Principal species in the system: calmodulin $+Mg^{2+} + Ca^{2+} +$ target(P).

comes more biphasic, reflecting the dominant effect of the C-domain specificity, and the enhancement of this by Mg^{2+}.

Figure 6 shows the effect of varying free $[Ca^{2+}]$ on the apparent target affinity for the two peptides in the presence and absence of 5 mM Mg^{2+}. These curves are calculated from (1) measured values of the stoichiometric association constants for Ca^{2+} ($K_1 - K_4$) in the presence and absence of either target peptide; (2) values of the stoichiometric association constants for Mg^{2+} estimated from the measured K_{av} values using the simplifying assumption that the two sites within each domain are identical; and (3) the measured affinity of either peptide for apo-CaM (all measurements in 100 mM KCl at pH 8). The curves show the target specific Ca^{2+} sensitivity of the affinity of the interactions, with limiting values of K_p approaching 10^{12} M^{-1} and 10^7 M^{-1} for WFF_p and NM2, consistent with measured values (Martin et al., 1999, and this work). Also, over a 100-fold range of $[Ca^{2+}]$ corresponding to the typical stimulation (pCa 7 to 5), the presence of Mg^{2+} has a marked effect in reducing K_{app} by 1.4 log units ($\times$25) for WFF_p and 0.6 log units (4$\times$) for NM2. These differences indicate the practical range of modulation by Mg^{2+}, which can be produced for a target (WFF_p) in which both domains interact with Ca–CaM (hence, there is a strong effect of Mg^{2+} on the N-domain interaction with the target sequence) and for a different sequence (NM2), which interacts preferentially with the C-domain (and hence the N-domain effect is lacking). Thus, the sensitivity of a Ca^{2+}-dependent target interaction to the presence of Mg^{2+} ion can provide information about whether one or more domains of CaM are involved. For example, the lesser effect of Mg^{2+} on CaM interaction with caldesmon site A peptide, compared with the larger effects with sk-MLCK and PDE (Ohki et al., 1997), suggests that it is the C-domain of CaM that interacts with this portion of the caldesmon target protein.

Discussion

In addressing the question of how the presence of Mg^{2+} affects the interactions of CaM with target sequences, we have sought to rationalize some of the apparent differences in the literature regarding the interactions of Mg^{2+} with CaM itself. In this regard, the intrinsic instability of apo-CaM, and the subsequent sensitivity of its conformation to solution conditions such as temperature and ionic strength mean that these factors have to be controlled to allow quantitative deductions to be made on effects that are specific to divalent ion binding. We have concentrated on elucidating when the binding of Mg^{2+} causes observable effects in terms of conformational or spectroscopic differences. These are found generally to occur in the physiological range of $[Mg^{2+}]$ (1–5 mM; i.e., much greater than the estimated concentration of cytoplasmic CaM ($\sim$10 μM; Persechini & Cronk, 1998). In view of the affinities involved, the studies reported here do not allow a definite assessment of the stoichiometry of Mg^{2+} interactions. The effects we report are consistent with Mg^{2+} binding at the same four sites as Ca^{2+}, as indicated by specific Mg^{2+}-dependent site-related signals in NMR studies (Seamon, 1980; Tsai et al., 1987; Ohki et al., 1997; Ouyang & Vogel, 1998). Experiments with the isolated N-domain of CaM (Malmendal et al., 1998) show that Mg^{2+} binds with threefold higher affinity to site I, where it perturbs residue I27 (cf. perturbation of I27, and the analogous residues I63, I100, and V136 on occupancy of sites I–IV by Ca^{2+} (Biekofsky et al., 1998; Biekofsky & Feeney, 1998). In the present work, spectrophotometric titration with Mg^{2+} indicates occupancy of sites in the N- and C-domains of CaM with K_{av} 570 and 180 M^{-1}. However, we cannot exclude the possibility that other external sites can be involved in additional Mg^{2+} binding, as suggested by mass spectrometry and calorimetry (Milos et al., 1986; Lafitte et al., 1995; Gilli et al., 1998).

We therefore now discuss the effect of the direct substitution of Mg^{2+} for Ca^{2+} in an EF-hand site of CaM in terms of (1) the likely conformational consequences in the immediate vicinity of the ion and beyond, and (2) the possible functional effect in target interactions.

The main effect of replacement of Ca^{2+} by Mg^{2+} in EF-hand structures appears to be the change from seven- (or higher) coordination of the metal ion to a more regular six-coordinated octahedral liganding (Falke et al., 1994). The conformational adjustment involves mainly the ligand from position 12 of the canonical EF-hand binding loop. In CaM, this is a strongly conserved glutamate residue (Falke et al., 1994), which is the second residue of the outgoing "F-helix." This residue provides bidentate (-Z-axis) ligation to Ca^{2+} in each of the four EF-hands of CaM, and this binding is coupled to the conformational change of a given domain from

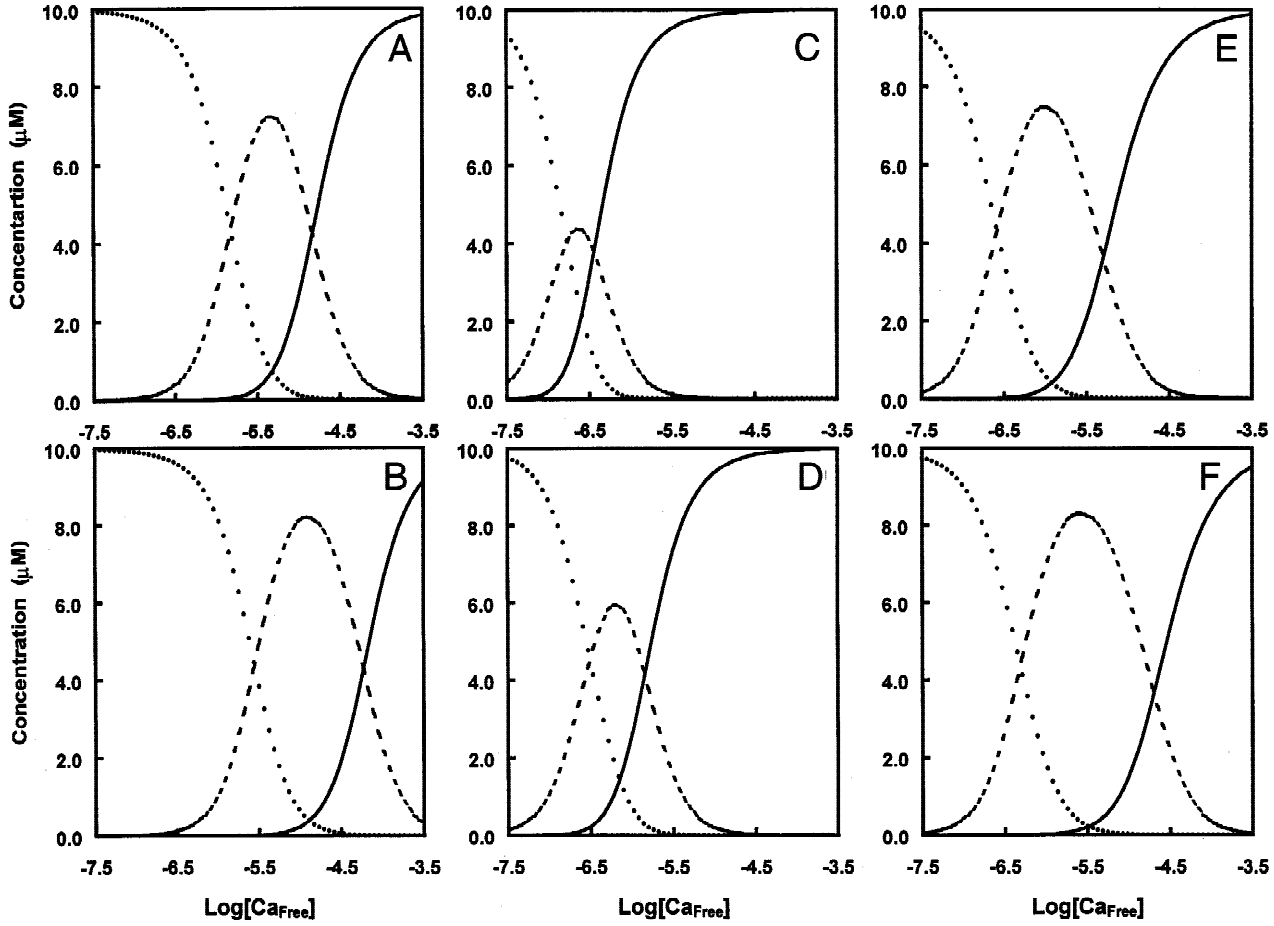

Fig. 5. Computer simulation of Ca^{2+} saturation curves. Concentrations of species containing zero (dotted lines), two (dashed lines), and four (solid lines) calcium ions calculated for: (**A**) CaM, (**B**) CaM in 5 mM Mg^{2+}, (**C**) CaM + WFF_p, (**D**) CaM + WFF_p in 5 mM Mg^{2+}, (**E**) CaM + NM2, (**F**) CaM + NM2 in 5 mM Mg^{2+}. The curves were calculated for 10 μM CaM plus 25 μM peptide using the stoichiometric association constants given in the text. The constants for CaM alone ($\log K_1 = 5.23$, $\log K_2 = 6.42$, $\log K_3 = 4.33$, $\log K_4 = 5.33$) were taken from Martin et al. (1996).

the apo "closed" form, to the holo "open" form (Finn et al., 1995; Kuboniwa et al., 1995; Zhang et al., 1995). This change is most readily represented as a modification in the interhelical angle of the two helices of a given EF-hand (see also Yap et al., 1999, for intermediate examples). It is the open form that has the hydrophobic exposure used in target recognition and interaction by Ca-CaM (Crivici & Ikura, 1995).

It appears that -Z liganding in an EF-hand is a potential determinant for either local or more global conformational effects. CD and NMR data show that binding of Mg^{2+} to CaM induces little of the global conformational effect produced by Ca^{2+} binding, but fluorescence data suggest that Mg^{2+} binding does cause local effects on binding loop residues in both domains. NMR structures of apo-CaM (1cfd.pdb, 1dmo.pdb) show the close proximity of the side chains of Tyr138 and Glu139, which could be responsible for the highly quenched tyrosine fluorescence emission (cf. Kilhoffer et al., 1981; Pundak & Roche, 1984). Several high-resolution Ca-CaM structures (e.g., 1osa.pdb and 4cln.pdb), show that the bidentate Ca^{2+} binding to Glu140 is accompanied by the displacement of Tyr138 from Glu139 toward Glu82, and Ca-CaM shows a normal intense fluorescence emission spectrum. We postulate that (even monodentate) liganding of Glu140 by Mg^{2+} could account for the similar (but smaller) increase in fluorescence emission observed upon Mg^{2+} binding. In Ca^{2+}-binding site I (N-domain), ligation of Mg^{2+} by Glu31 and by the polypeptide carbonyl of residue 7 in the loop (T26 in WT CaM) causes a change in the local environment as monitored by NMR of Thr26 (Malmendal et al., 1999) and Ile27 (Ohki et al., 1997). This could account for the observed Mg^{2+}-induced change in the fluorescence emission of the substituted Trp residue at position 26 in the T26W syncam mutant.

X-ray data are not available for Mg^{2+} bound to CaM, but high-resolution structures exist for Ca^{2+} and Mg^{2+} bound to the archetypal EF-hand of parvalbumin. These structures show that when bidentate Ca^{2+} is replaced by monodentate Mg^{2+}, there is very little effect on the conformation and interhelical angle of the parvalbumin EF-hand pair, which remains in the normal "open" form (4pal.pdb; Declercq et al., 1991). In a parvalbumin mutant with a Glu to Asp substitution at position 12 of Ca^{2+}-binding site I, Mg^{2+} binding causes a translation of 1.1A in the position of the F-helix (1b8c.pdb; Cates et al., 1999), showing again that Mg^{2+} can be fully six-coordinated in an EF hand. However, the function of parvalbumin is thought to be that of a Ca^{2+} buffer rather than a Ca^{2+} sensor or trigger (Ikura, 1996), and the open conformation is

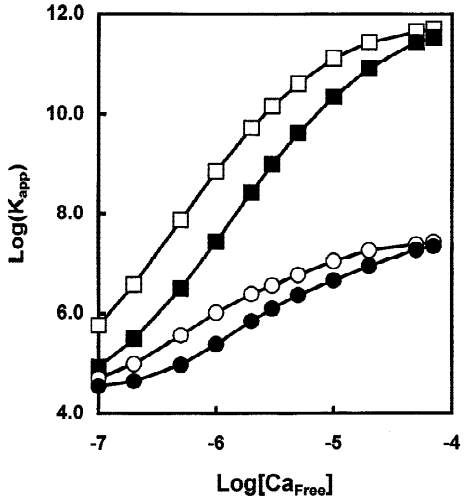

Fig. 6. Mg^{2+} effects on target affinity. The effect of Mg^{2+} on the apparent affinity (K_{app}, M^{-1}) of CaM for the target peptides WFF_p (squares) and NM2 (circles) as a function of free [Ca^{2+}]. Open symbols, no Mg^{2+}; closed symbols, 5 mM Mg^{2+}. Calculations were performed as described in the text.

apparently not associated with target interactions. In the case of CaM, mutation of Glu to Gln or Lys in position 12 of any of the Ca^{2+}-binding loops has been shown to affect Ca^{2+} affinity and domain conformation (Martin et al., 1992; Maune et al., 1992a, 1992b), but does not necessarily prevent target interactions, which can occur with reduced affinity (cf. Haiech et al., 1991; Findlay et al., 1995). The effect of mutating the Glu at position 12 of the loop to Gln has been investigated in detail by the Forsén group, and in the case of site IV, evidence exists for the loop adopting a multiplicity of conformations in dynamic interchange (Evenäs et al., 1997).

Thus, the question arises: does Mg-CaM represent the conformation of apo-CaM, but with Mg^{2+} ligated (possibly monovalently) in the usual Ca^{2+} sites? The resemblance between the two is found in (1) far-UV CD spectra (Fig. 1A, curves Mg and K) indicating a similar (stable) secondary structure; (2) the absence of hydrophobic exposure in either domain with Mg^{2+}; and (3) the similarity in near-UV CD and absorption spectra (Fig. 1B,C; curves Mg and K). Differences are shown in (1) the NMR spectra; and (2) and in the fluorescence of Tyr138 (Fig. 1D, curves Mg and K), both markedly different from the emission spectrum of apo-CaM. These results lead us to postulate that apo-CaM and Mg-CaM are probably similar in the globular portion of each domain containing the hydrophobic core (which is not exposed to solvent), but with a more specific conformation to the loop sequences bound to Mg^{2+} than the flexible empty binding loops of apo-CaM. The binding of Mg^{2+} has the additional effect of stabilizing both domains against thermal denaturation (Tsalkova & Privalov, 1985) and recent studies of chemical denaturation (Masino et al., 2000) show that the stabilizing effect is greater in the N-domain, consistent with the higher K_{av} of this domain for Mg^{2+}. Thus, 5 mM Mg^{2+} increases the stabilities of the N- and C-domains of CaM at 20 °C by ~1.4 and 0.6 kcal/mol. It is therefore likely that physiological [Mg^{2+}] helps to ensure that CaM is largely in the Mg^{2+}-bound form under "Ca^{2+}-free" conditions. Presumably this helps to protect against possible thermal or enzymatic degradation, and further protection may result from interaction with Ca^{2+}-independent targets such as neuromodulin.

It is well established that Mg^{2+} does not substitute for Ca^{2+} in promoting the CaM-dependent activation of target enzymes, and this selectivity is the basis of the Ca^{2+}-dependent physiological response. However, the ability of Mg^{2+} to compete with Ca^{2+} suggests that it can exert a modulating effect in the regulation of CaM–target interactions. In previous work, we have investigated the nature of the species generated as a result of the response of CaM to changing [Ca^{2+}]. It was suggested that a species of intermediate calcium saturation (Ca_2-CaM-target), involving occupancy of the C-domain sites may function under both equilibrium and kinetic conditions as an inactive but readily activatable intermediate, with a role in the regulatory process (Bayley et al., 1996; Brown et al., 1997). The existence of such a species is due to the difference in average affinity (and corresponding rate constants) for Ca^{2+} binding to the two domains, deriving from the significant differences that exist in the otherwise highly conserved loop sequences. The presence of Mg^{2+} has a different effect on the Ca^{2+} affinity of each domain. The values of K_{av} for Mg^{2+} binding to either domain derived from competition studies using the indicator method agree well with the values obtained from direct Mg^{2+} titrations. Hence, we deduce that these affinities correspond to Mg^{2+} binding processes that cause the small but specific conformational effects in the binding loops of both domains. These values also agree with earlier work in showing that Mg^{2+} binds significantly more tightly to the N-domain. The result is that the intrinsic differences in the average Ca^{2+} affinity of the two domains is significantly amplified in the presence of Mg^{2+}.

The simulation of a relatively simple mechanism of competition of Ca^{2+} and Mg^{2+} for the normal binding sites illustrates the magnitude of the modulating influence of Mg^{2+} that can be generated by this mechanism. Any such competition clearly attenuates the apparent increase in Ca^{2+} affinity of CaM in the presence of a (Ca^{2+}-dependent) target sequence. In addition, Ca^{2+} binds preferentially to the C-domain, whereas Mg^{2+} binds preferentially to the N-domain. Thus, the optimal proportion of the intermediate Ca_2-CaM-target complex is increased by the presence of Mg^{2+}, and this occurs in a target specific way. This adds a further degree of versatility in the domain specificity of CaM-target interactions.

In conclusion, the biological effect of Mg^{2+} is significant in two main respects: first, Mg^{2+} increases the thermodynamic stability of both domains of CaM, decreasing the fraction of unfolded protein potentially present under physiological conditions. Thus, a primary role of Mg^{2+} could be the avoidance of CaM in a truly apo state in which it would be vulnerable to unfolding and proteolytic cleavage (Mackall & Klee, 1991). Second, the opposite differential affinities of Ca^{2+} and Mg^{2+} for the N- and C-domains of CaM mean that the domain specificity in the Ca^{2+}-dependent interaction of CaM with a given target sequence can be modulated by Mg^{2+}. The target preference is normally for the C-domain, and this can be further enhanced by persistence of the Ca_2-CaM-target complex at higher [Ca^{2+}] due to the fact that Mg^{2+} competes more effectively with Ca^{2+} for binding to the N-domain. If a particular target sequence selectively increased the Mg^{2+} affinity of the N-domain, then such effects could be enhanced still further. By contrast, in the case where the target sequence interacts only with the C-domain, the modulating effects of Mg^{2+} vs. Ca^{2+} are expected be less significant. In the case of "Ca^{2+}-independent" target interactions, the present work indicates that it is important to evaluate affinities of target not simply for Ca^{2+}-free CaM, but also

for Ca^{2+}-free CaM in the presence of Mg^{2+}, because in physiological concentrations of Mg^{2+}, apo-CaM is largely converted into the Mg^{2+}-bound form.

Materials and methods

Proteins and peptides

Drosophila CaM was expressed in *Escherichia coli* and purified as described (Browne et al., 1997). CaM was made Ca^{2+}-free by incubating with 15 mM EGTA and then desalting by passage though two Pharmacia PD10 (G25) columns equilibrated with Chelex-treated buffer (25 mM Tris, 100 mM KCl, pH 8.0). The peptides WFF_p (Ac-KRRWKKNFIAVSAANRFK-NH_2) and NM2 (Ac-ATKWQASFRGHITRKKLKG-NH_2) were prepared as described (Findlay et al., 1995). WFF_p is the first 18 residues of M13, the CaM target sequence of sk-MLCK; NM2 corresponds to part of the target sequence of neuromodulin with an I4W substitution. Concentrations were determined spectrophotometrically using $\epsilon_{280} =$ 5,690 $M^{-1}\,cm^{-1}$ for the peptides (Gill & von Hippel, 1989) and $\epsilon_{279} =$ 1,578 $M^{-1}\,cm^{-1}$ for Ca-CaM (Maune et al., 1992b).

Optical spectra

Near- and far-UV CD spectra of CaM were recorded on a JASCO J-715 spectropolarimeter as described (Findlay et al., 1995; Bayley et al., 1996). Spectra are presented as the CD absorption coefficient calculated using the molar concentration of CaM ($= \Delta\epsilon_M$) rather than on a mean residue weight (mrw) basis. Values of $\Delta\epsilon_{mrw}$ may be calculated as $\Delta\epsilon_{mrw} = \Delta\epsilon_M/N$, where N is the number of peptide bonds ($= 146$ for CaM). Absorption spectra were recorded using a Cary 3E spectrophotometer. Uncorrected tryptophan emission spectra were recorded using a SPEX FluoroMax fluorimeter with $\lambda_{ex} = 280$ or 290 nm (bandwidth 1.7 nm) and emission from 310 to 450 nm (bandwidth 5 nm). Spectra were recorded in 25 mM Tris (pH 8.0) with added KCl, $CaCl_2$, and $MgCl_2$ as appropriate. Buffers for measurements in the absence of Ca^{2+} contained some EGTA ($\sim$20 μM) to ensure the complete absence of Ca^{2+}. Spectra were recorded at 20° unless otherwise noted.

Calcium binding studies

The stoichiometric Ca^{2+} association constants for CaM in the presence and absence of Mg^{2+} (1–10 mM) were determined from Ca^{2+} titrations of apo-CaM performed in the presence of the chelator 5,5′-Br_2BAPTA, using published methods (Linse et al., 1991; Martin et al., 1996). Measurements were made at 20 °C in 10 mM Tris, 100 mM KCl, pH 8.0. The presence of Mg^{2+} does not interfere with the assay, because the association constant of the chelator with Mg^{2+} is $<5\ M^{-1}$ under these conditions (S.R. Martin, unpubl. obs.; cf. Pethig et al., 1989). Titrations of apo-CaM in the presence of excess NM2 or WFF_p were performed using 5,5′-Br_2BAPTA or Quin 2, as described elsewhere (Bayley et al., 1996).

For an isolated CaM domain (with two stoichiometric calcium association constants, K_1 and K_2), it is convenient to define an average (or mean) calcium affinity as $K_{av(Ca)} = (K_1K_2)^{0.5}$. The reciprocal of $K_{av(Ca)}$ is the free Ca^{2+} concentration at the midpoint of the saturation curve. If Mg^{2+} competes directly with Ca^{2+} for the two available sites, then the average Ca^{2+} affinity measured in the presence of a fixed concentration of Mg^{2+} should be equal to $K^C_{av(Ca)}/(1 + K^C_{av(Mg)})$ for the isolated C-domain and $K^N_{av(Ca)}/(1 + K^N_{av(Mg)})$ for the isolated N-domain (Malmendal et al., 1999). In the case of intact CaM, the situation is more complex because there are four stoichiometric constants to be considered. However, the C-domain of CaM binds Ca^{2+} more strongly than the N-domain, and it is easy to show (Linse et al., 1991) that the average affinity of the C-domain for Ca^{2+}, $K^C_{av(Ca)}$, is approximately equal to $(K_1K_2)^{0.5}$, while the average affinity of the N-domain for Ca^{2+}, $K^N_{av(Ca)}$, is approximately equal to $(K_3K_4)^{0.5}$. The effects of Mg^{2+} on the average Ca^{2+} affinities of the two domains in intact CaM may then be assessed in the same way as for an isolated domain.

Determination of peptide affinities

Dissociation constants for WFF_p and NM2 were determined by direct fluorometric titration of the peptide with CaM in 25 mM Tris at pH 8.0 as described elsewhere (Findlay et al., 1995).

Acknowledgments

We thank Dr. J. Haiech (Marseille) for providing us with the T26W mutant of syncam, and Peter Browne for preparation of *Drosophila* CaM.

References

Bayley PM, Findlay WA, Martin SR. 1996. Target recognition by calmodulin: Dissecting the kinetics and affinity of interaction using short peptide sequences. *Protein Sci 5*:1215–1228.

Berridge MJ, Bootman MD, Lipp P. 1998. Calcium—A life and death signal. *Nature 395*:645–648.

Biekofsky RR, Feeney J. 1998. Cooperative cyclic interactions involved in metal binding to pairs of sites in EF-hand proteins. *FEBS Lett 439*:101–106.

Biekofsky RR, Martin SR, Browne JP, Bayley PM, Feeney J. 1998. Ca^{2+} coordination to backbone carbonyl oxygen atoms in calmodulin and other EF-hand proteins: ^{15}N chemical shifts as probes for monitoring individual-site Ca^{2+} coordination. *Biochemistry 37*:7617–7629.

Brown SE, Martin SR, Bayley PM. 1997. Kinetic control of the dissociation pathway of calmodulin–peptide complexes. *J Biol Chem 272*:3389–3397.

Browne JP, Strom M, Martin SR, Bayley PM. 1997. The role of β-sheet interactions in domain stability, folding, and target recognition reactions of calmodulin. *Biochemistry 36*:9550–9561.

Cates MS, Berry MB, Ho EL, Li Q, Potter JD, Phillips GN. 1999. Metal-ion affinity and specificity in EF-hand proteins: Coordination geometry and domain plasticity in parvalbumin. *Structure 7*:1269–1278.

Crivici A, Ikura M. 1995. Molecular and structural basis of target recognition by calmodulin. *Annu Rev Biophys Biomol Struct 24*:85–116.

Declercq J-P, Tinant B, Parello J, Rambaud J. 1991. Ionic interactions with parvalbumins. Crystal structure determination of pike 4.10 parvalbimun in four different ionic environments. *J Mol Biol 220*:1017–1039.

Drabikowski W, Brzeska H, Venyaminov SY. 1982. Tryptic fragments of calmodulin. Ca^{2+}- and Mg^{2+}-induced conformational changes. *J Biol Chem 257*:1584–11590.

Ebel H, Gunther T. 1980. Magnesium metabolism: A review. *J Clin Chem Clin Biochem 18*:257–270.

Evenäs J, Thulin E, Malmendal A, Forsén S, Carlstrom G. 1997. NMR studies of the E140Q mutant of the carboxy-terminal domain of calmodulin reveal global conformational exchange in the Ca2+-saturated state. *Biochemistry 36*:3448–3457.

Falke JJ, Drake SK, Hazard AL, Peersen OB. 1994. Molecular tuning of ion binding to calcium signaling proteins. *Q Rev Biophys 27*:219–290.

Findlay WA, Martin SR, Beckingham K, Bayley PM. 1995. Recovery of native structure by calcium binding site mutants of calmodulin upon binding of sk-MLCK target peptides. *Biochemistry 34*:2087–2094.

Finn BE, Evanäs J, Drakenberg T, Waltho JP, Thulin E, Forsén S. 1995. Calcium-induced structural changes and domain autonomy in calmodulin. *Nat Struct Biol 2*:777–783.

Follenius A, Gerard D. 1984. Fluorescence investigations of calmodulin hydrophobic sites. *Biochem Biophys Res Commun 119*:1154–1160.

Gill SC, von Hippel PH. 1989. Calculation of protein extinction coefficients from amino acid sequence data. *Anal Biochem 182*:319–326.

Gilli R, Lafitte D, Lopez C, Kilhoffer M-C, Makarov A, Briand C, Haiech J. 1998. Thermodynamic analysis of calcium and magnesium binding to calmodulin. *Biochemistry 37*:5450–5456.

Haiech J, Kilhoffer MC, Lukas TJ, Craig TA, Roberts DM, Watterson DM. 1991. Restoration of the calcium binding activity of mutant calmodulins toward normal by the presence of a calmodulin binding structure. *J Biol Chem 266*:3427–2431.

Haiech J, Klee CB, Demaille JG. 1981. Effects of cations on affinity of calmodulin for calcium: Ordered binding of calcium ions allows the specific activation of calmodulin-stimulated enzymes. *Biochemistry 20*:3890–3897.

Houdusse A, Silver M, Cohen C. 1996. A model of Ca^{2+}-free calmodulin binding to unconventional myosins reveals how calmodulin acts as a regulatory switch. *Structure 4*:1475–1490.

Ikura M. 1996. Calcium binding and conformational response in EF-hand proteins. *Trends Biochem Sci 21*:14–17.

Kilhoffer M-C, Demaille JG, Gerard D. 1981. Tyrosine fluorescence of ram testis and octopus calmodulins. Effects of calcium, magnesium, and ionic strength. *Biochemistry 20*:4407–4414.

Kilhoffer M-C, Kubina M, Travers F, Haiech J. 1992. Use of engineered proteins with internal tryptophan reporter groups and perturbation techniques to probe he mechanism of ligand protein interactions: Investigation of the mechanisms of calcium binding to calmodulin. *Biochemistry 31*:8098–8106.

Kuboniwa H, Tjandra N, Grzesiek S, Ren H, Klee CB, Bax A. 1995. Solution structure of calcium-free calmodulin. *Nat Struct Biol 2*:768–776.

Lafitte D, Capony JP, Grassy, G, Haiech J, Calas B. 1995. Analysis of the ion binding sites of calmodulin by electrospray ionization mass spectrometry. *Biochemistry 34*:13825–13832.

Linse S, Helmersson A, Forsén S. 1991. Calcium binding to calmodulin and its globular domains. *J Biol Chem 266*:8050–8054.

Mackall J, Klee CB. 1991. Calcium-induced sensitization of the central helix of calmodulin to proteolysis. *Biochemistry 30*:7242–7247.

Malmendal A, Evenäs J, Thulin E, Gippert GP, Drakenberg T, Forsén S. 1998. When size is important. Accommodation of magnesium in a calcium binding regulatory domain. *J Biol Chem 273*:28994–29001.

Malmendal A, Linse S, Evenäs J, Forsén S, Drakenberg T. 1999. Battle for the EF-hands: Magnesium–calcium interference in calmodulin. *Biochemistry 38*:11844–11850.

Martin SR, Bayley PM. 1986. The effect of Ca^{2+} and Cd^{2+} on the secondary and tertiary structure of calmodulin. *Biochem J 238*:485–490.

Martin SR, Bayley PM, Brown SE, Porumb T, Zhang M, Ikura M. 1996. Spectroscopic characterization of a high-affinity calmodulin-target peptide hybrid molecule. *Biochemistry 35*:3508–3517.

Martin SR, Lu AQ, Xiao J, Kleinjung J, Beckingham K, Bayley PM. 1999. Conformational and metal-binding properties of androcam, a tetsis-specific, calmodulin-related protein from *Drosophila*. *Protein Sci 8*:2444–2454.

Martin SR, Maune JF, Beckingham K, Bayley PM. 1992. Calcium dissociation from calcium binding site mutants of *Drosophila melanogaster* calmodulin: Stopped-flow studies. *Eur J Biochem 205*:1107–1114.

Masino L, Martin SR, Bayley PM. 2000. Ligand binding and thermodynamic stability of a multi-domain protein, calmodulin. *Protein Sci 9*:1519–1529.

Maune JF, Beckingham K, Martin SR, Bayley PM. 1992a. Circular dichroism studies on calcium binding to two series of Ca^{2+} binding site mutants of *Drosophila melanogaster* calmodulin. *Biochemistry 31*:7779–7786.

Maune JF, Klee CB, Beckingham K. 1992b. Ca^{2+} binding and conformational change in two series of point mutations to the individual Ca^{2+}-binding sites of calmodulin. *J Biol Chem 267*:5286–5295.

Milos M, Schaer J-J, Comte M, Cox JA. 1986. Calcium–proton and calcium–magnesium antagonisms in calmodulin: Microcalorimetric and potentiometric analyses. *Biochemistry 25*:6279–6287.

Ohki S-Y, Ikura M, Zhang M. 1997. Identification of Mg^{2+}-binding sites and the role of Mg^{2+} on target recognition by calmodulin. *Biochemistry 36*: 4309–4316.

Ouyang H, Vogel HJ. 1998. Metal ion binding to calmodulin: NMR and fluorescence studies. *Bioessays 11*:213–222.

Peersen PB, Madsen TS, Falke JJ. 1997. Intermolecular tuning of calmodulin by target peptides and proteins: Differential effects on Ca^{2+} binding and implications for kinase activation. *Protein Sci 6*:794–807.

Persechini A, Cronk B. 1998. The relationship between the free concentrations of Ca^{2+} and Ca^{2+}-calmodulin in intact cells. *J Biol Chem 274*:6827–6830.

Pethig R, Kuhn, M, Payne R, Adler E, Chen T-H, Jaffe LF. 1989. On the dissociation constants of BAPTA-type calcium buffers. *Cell Calcium 10*:491–498.

Pundak S, Roche RS. 1984. Tyrosine and tyrosinate fluorescence of bovine testes calmodulin: Calcium and pH dependence. *Biochemistry 23*:1549–1555.

Seamon KB. 1980. Calcium- and magnesium-dependent conformational states of calmodulin as determined by nuclear magnetic resonance. *Biochemistry 19*:207–215.

Tsai M-D, Drakenberg T, Thulin E, Forsén S. 1987. Is the binding of magnesium(II) to calmodulin significant—An investigation by magnesium-25 nuclear-magnetic-resonance. *Biochemistry 26*:3635–3643.

Tsalkova TN, Privalov PL. 1985. Thermodynamic study of domain organization in troponin C and calmodulin. *J Mol Biol 181*:533–544.

Tsvetkov PO, Prostasevich II, Gilli R, Lafitte D, Lobachov VM, Haiech J, Briand C, Makarov AA. 1999. Apocalmodulin binds to the myosin light chain kinase calmodulin target site. *J Biol Chem 274*:18161–18164.

Yap KL, Ames JB, Swindells MB, Ikura M. 1999. Diversity of conformational states and changes within the EF-hand protein superfamily. *Proteins 37*: 499–507.

Zhang M, Tanaka T, Ikura M. 1995. Calcium-induced conformational transition revealed by the solution structure of apo–calmodulin. *Nat Struct Biol 2*:758–767.